Ecological Indicators 89 (2018) 199–212

Contents lists available at ScienceDirect

Ecological Indicators

journal homepage: www.elsevier.com/locate/ecolind

Indicator-based assessment of post-fire recovery dynamics using satellite NDVI time-series

Torres João*, Gonçalves João, Marcos Bruno, Honrado João

InBIO – Rede de Investigação em Biodiversidade e Biologia Evolutiva, Laboratório Associado/CIBIO – Centro de Investigação em Biodiversidade e Recursos Genéticos, Faculdade de Ciências, Universidade do Porto, Campus Agrário de Vairão, 4485-601 Vairão, Portugal

ARTICLE INFO

Keywords:
MODIS
NDVI
Post-fire recovery
Remote sensing
Time series
Vegetation indices
Wildfires

ABSTRACT

Fire disturbance severely modifies ecosystem structure and functioning, and therefore predicting post-fire responses is pivotal to improve land management. Indicators that efficiently link post-fire recovery with a timely decision on landscape management can play a key role in the governance of fire risk. We describe a framework to evaluate post-fire recovery based on remotely-sensed measures of relative vegetation recovery, calculated from satellite NDVI time-series. Three indicators are proposed: the novel Cumulative Relative Recovery Index (CRRI), measuring the (mid-long term) extent and completeness of recovery; the Recovery Trend Index (RTI), measuring the steepness of the mid-term post-fire recovery trend; and the Half Recovery Time index (HRT), a measure of the short-term recovery rate. We used Random Forest (RF) models to predict the observed recovery patterns and ranked the predictive importance of several candidate explanatory factors. The performance of RF models ranged from good (CRRI, RTI) to moderate (HRT). Three sets of predictive variables consistently ranked higher: fire traits, landscape composition, and post-fire climatic conditions. The relative contribution of individual variables was different across recovery indicators. These results show that proposed indicators seem to capture different facets of the post-fire recovery process. The short-term recovery indicator (HRT) was linked to landscape composition and post-fire climate. Thus, HRT expresses the speed of initial recovery, related to differences in fire-response traits of vegetation and to climatic conditions immediately following fire. The mid-term recovery indicator (RTI) was mainly influenced by fire traits and post-fire climatic conditions. This indicator captures multiple interacting effects that shape the recovery process related to fire severity, vegetation type and post-fire conditions. Finally, the long-term recovery indicator (CRRI) was clearly more influenced by fire attributes related to severity than by vegetation type and structure or by post-fire climatic conditions. Overall, our results suggest that a combination of biotic processes (driven by plant life-history traits) and abiotic filters (e.g., post-fire climate) determine the early post-fire recovery process. Conversely, the mid to long-term recovery response (expressing its completeness) is driven by the depletion of resilience capacity and by the amount of change in vegetation structure and functioning modulated by spatial differences in fire severity. Our results strongly suggest that an indicator-based approach grounded on satellite time-series of vegetation indices can effectively cover various facets of post-fire recovery. This will improve the monitoring and prediction of post-fire recovery dynamics, with valuable applications in fire hazard management and post-fire ecosystem restoration and monitoring.

1. Introduction

The field of fire ecology has evolved to include an ever broader range of concepts and techniques (Keeley et al., 2011). Traditionally, fire research emphasised the relation between wildfire patterns and structural features of the landscape, such as land cover categories (Bajocco and Ricotta, 2008; Nunes et al., 2005) or vegetation types (Gumming, 2001; Krivtsov et al., 2009). This focus has been shifting towards the links of fire with various functional characteristics of vegetation, such as productivity dynamics or fuel phenology, in order to early detect or even anticipate ecosystem changes (Alcaraz-Segura et al., 2008; Angelis et al., 2012). This functional approach can be particularly useful in areas of the globe under a Mediterranean climate, with a marked seasonality of wildfire occurrence (Bajocco and Ricotta, 2008; Beven and Germann, 2013; Helman et al., 2015; Pausas, 2004) and a strong relation between the seasonal timing of vegetation and wildfire regimes (Bajocco et al., 2010).

Changes in ecosystem and landscape functioning induced by fire

* Corresponding author.
E-mail address: joao.torres@fc.up.pt (T. João).

https://doi.org/10.1016/j.ecolind.2018.02.008
Received 27 February 2017; Received in revised form 16 January 2018; Accepted 2 February 2018
1470-160X/ © 2018 Published by Elsevier Ltd.

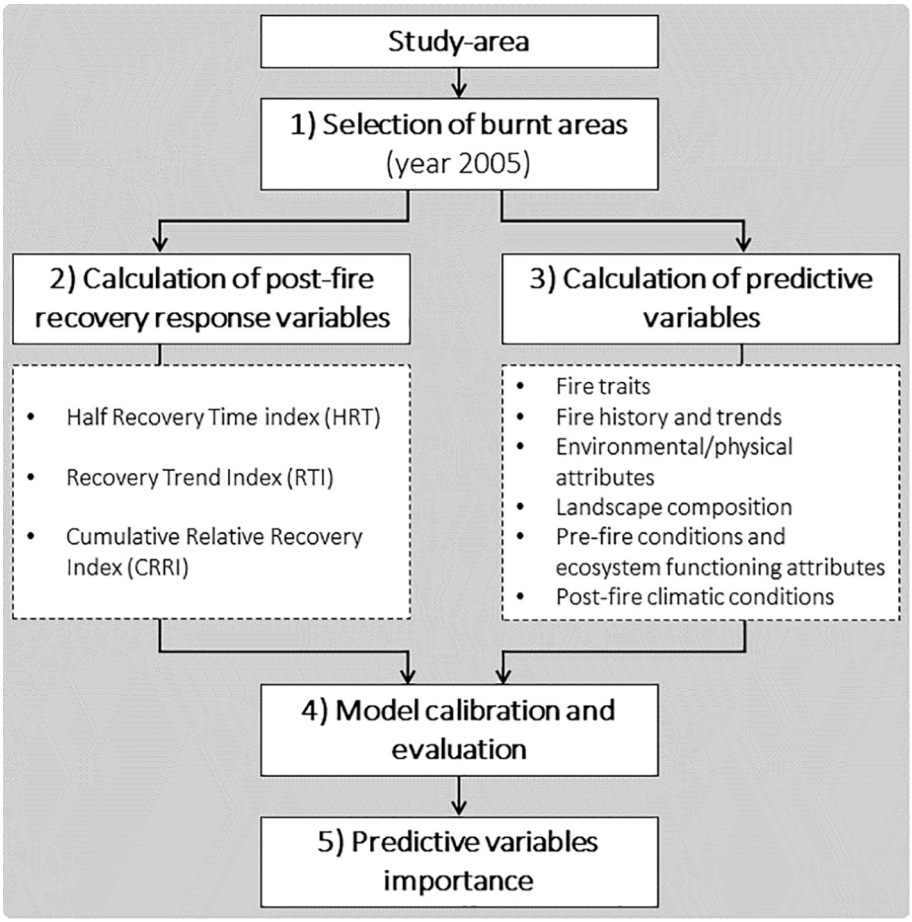

Fig. 1. Diagram representation of the general workflow adopted for the analysis of post-fire vegetation recovery.

disturbance have been reported from studies based on satellite imagery and remote sensing methods. Those changes include drastic decreases of photosynthetic activity (e.g. Gouveia et al., 2010; Tonbul et al., 2016), shifts in vegetation phenology (e.g. Angelis et al., 2012), changes in structure and function in forest landscapes (Cavallero et al., 2015), or feedbacks between surface temperature and climate change in burnt boreal forests (Rogers et al., 2012). Moreover, remote sensing of vegetation offers comprehensive spatiotemporal information about properties and condition of fuel type (Angelis et al., 2012; Schneider et al., 2008).

Remotely-sensed vegetation indices have also been used to analyse post-fire recovery. Díaz-Delgado et al. (2002) used the Normalized Difference Vegetation Index (NDVI) from Landsat imagery to monitor vegetation recovery after successive fires; they successfully correlated fire recurrence with resilience and with the contribution of different plant life strategies to that same resilience. van Leeuwen et al. (2010) used a remotely-sensed NDVI time-series to extract land surface phenological attributes (including the start and end of the growing season, the base and peak values, and the integrated seasonal NDVI), to monitor post-fire vegetation response. Di-Mauro et al. (2014) used MODIS-derived vegetation indices to analyse post-fire resilience and shifts in the start and end of the growing season, in broadleaf forest and prairies. The results from these and other studies suggest that satellite time-series of vegetation functioning data may support a valuable toolkit for efficiently monitoring post-fire responses. For example, remotely-sensed observations such as those obtained from the MODIS sensors provide comprehensive spatial coverage and enough temporal resolution (8 or 16-days composites of daily images) to update vegetation condition in a more efficient, timely and operational manner than traditional aerial photography (Oswald et al., 1999) or in-field surveillance (Riaño et al., 2002). These characteristics highlight the importance of developing remotely-sensed indicators for monitoring post-fire vegetation recovery. Indeed, satellite products have been particularly useful for investigating not only fire disturbances but also post-fire recovery (White et al., 2017). However, in spite of the accumulated evidence of the added-value of remote sensing to multiple aspects of fire ecology, there is still a lack of satellite-based indicator sets that can adequately describe different facets of post-fire vegetation recovery, namely concerning its rate and completeness. In this regard, three types of functional attributes potentially useful for tracking post-fire recovery can be extracted as yearly measures from NDVI time-series: productivity (annual mean), seasonality (annual range) and phenology (date of the maximum value) (Alcaraz et al., 2006). These three types of attributes describe the height and shape of the annual NDVI curve, and previous studies have shown they have biological significance (e.g., Alcaraz-Segura et al., 2017; Pettorelli et al., 2005).

Here we explored the usefulness of a high-temporal resolution satellite (MODIS) products to assess pre- and post-fire vegetation functioning dynamics. Specifically, we aimed to identify and rank the main drivers of the post-fire vegetation recovery process. Building on the Essential Variables narrative (e.g., Pettorelli et al., 2016), we explored a limited set of satellite-based indices to analyse post-fire recovery and its drivers in northern Portugal, a wildfire hotspot in Europe (EFFIS, 2015). First, we analysed pre- and post-fire NDVI profiles of a set of areas burnt in 2005, a focal year characterized by extreme wildfire occurrence (Marques et al., 2011). For each recovery indicator, we developed a predictive model to analyse how it is affected by fire severity, fire spatial attributes, fire history, physical environment, post-fire climatic conditions, landscape composition, and pre-fire vegetation functioning. Our final goal was to select a core set of indicators based

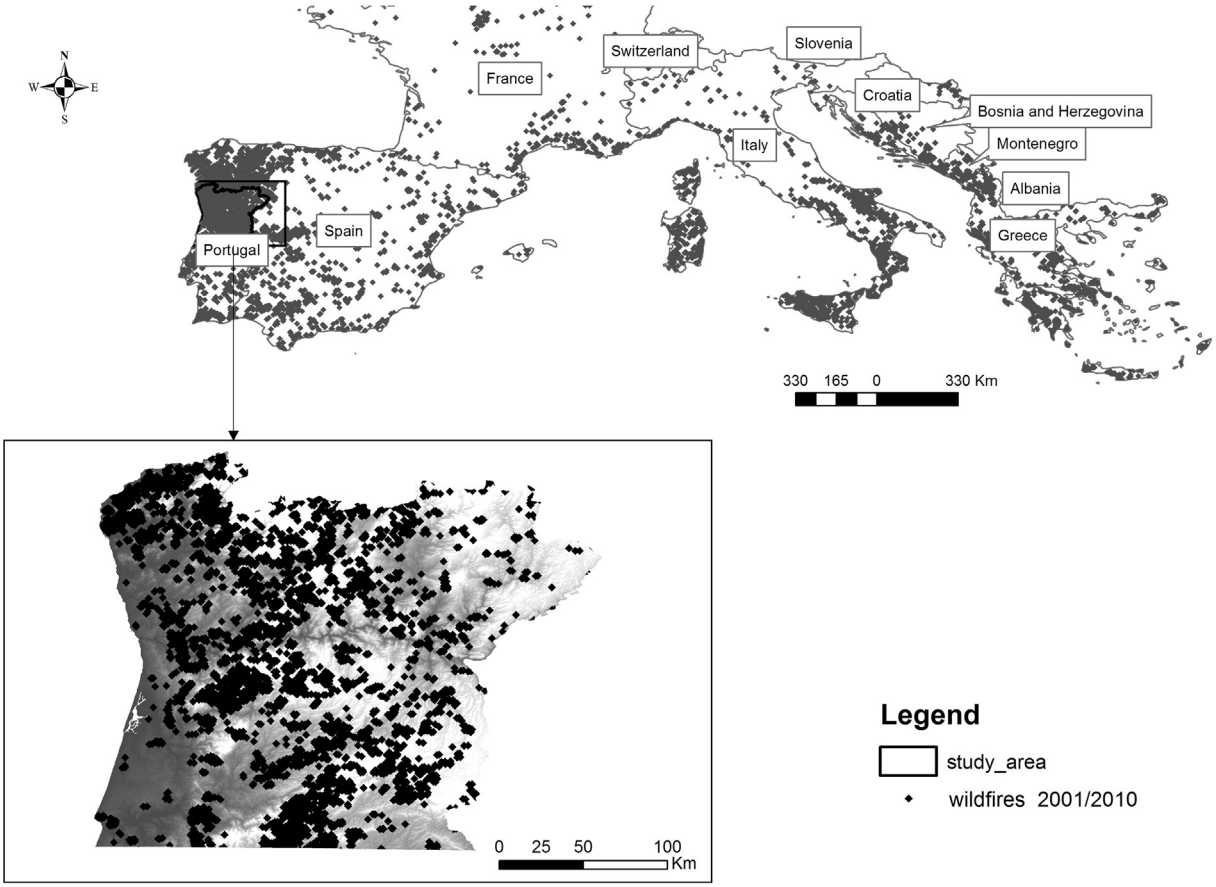

Fig. 2. Wildfires in Southern Europe and in the study area (northern Portugal) for the time frame 2001–2011; the study area is located in the highest fire incidence region of Europe (Northwest Iberian Peninsula). Source: EFFIS, 2015.

on remote-sensing vegetation indices to capture the different facets of vegetation recovery across a region heavily affected by wildfires and with high socio-environmental heterogeneity.

2. Material and methods

2.1. General approach and workflow

The general workflow included five sequential steps (Fig. 1), as described in the sections below: (1) selection of burnt areas for the focal year of 2005; (2) computation of post-fire recovery response variables (candidate indicators); (3) computation and pre-selection of predictive variables; (4) model calibration, evaluation and ranking; and (5) assessment of the importance of individual predictive variables.

2.2. Test area, wildfire data, and focal burnt areas

The studied area comprises the northern part of continental Portugal (Fig. 2), limited at south by the *Serra da Estrela* mountain range (upper left: −8.90°, 42.15°; lower right: −6.25°, 39.97°). This area includes the westernmost transition between the Atlantic and Mediterranean environmental zones and biogeographic regions of Europe (Costa et al., 1998; Metzger et al., 2005). There are wide variations in elevation (from 0 m to 1993 m) and a large heterogeneity of environmental conditions (climate, radiation, soil types). The continental Mediterranean climate in the inland areas contrasts with the Atlantic climate predominant towards west and in sub-coastal mountains (Costa et al., 1998). According to Corine Land Cover 2006 (Caetano et al., 2009), the study area is mainly composed by 4% of urban/artificial areas, 39% by agricultural and agroforestry land, 31% by combining scrubland and sparsely vegetated areas, 4% by natural and semi-natural grasslands and 21% is covered by forests.

This area has the highest frequency of wildfires in Portugal (Pereira et al., 2006) and one of the highest frequencies across southern Europe (EFFIS, 2015; Fig. 2). In Portugal, the annual burnt area has considerably increased during the last three decades. From 1980 to 2004, an area equivalent to 30% of the country was burnt. In the period between 2000 and 2011, the average yearly burnt area was above 150,000 hectares, and the average number of occurrences was ca. 25,000 per year (European Commission, 2010). These values are three and five times more than for Italy and Spain respectively (Pereira et al., 1998; Pereira and Santos, 2003).

Fire data for Portugal were available from the national forest authority (ICNF) in vector format, with a minimum mapping area of 5 hectares available between 1990 and 2011 (ICNF, 2016). A vector grid with a cell size of 250x250m (corresponding to the spatial resolution of MODIS data) was used to calculate the percentage of burnt area per year for each cell. Grid cells that burned 75% or more of their surface area in 2005 and that remained completely unburned or partially burned (up to a threshold of 25% or less) in the remaining years of the focal time period (2001–2011) were selected to analyse post-fire recovery.

2.3. Computation of response variables

Recovery indicators were calculated from the Terra/MODIS NDVI time-series product MOD13Q1. This includes composite data for every 16 days, with corrections for atmospheric effects such as clouds and aerosols, as well as a data quality assessment (QA) layer (Solano et al., 2010). Additional corrections were made to the time-series in order to

Table 1
List of selected variables related to Fire traits and to Fire history and recent trends in burnt area. Columns in the left display if the variable entered the final RF model for Cumulative Relative Recovery Index (CRRI), Recovery Trend Index (RTI) and Half Recovery Time (HRT).

CRRI	RTI	HRT	Variable acronym	Description
Fire traits				
x	x	x	BRGMI	NDVI post-fire break magnitude index calculated as difference between the median NDVI between 2001–2004 and the 2005 minimum NDVI
x	x	x	BPCRI	Burnt patch circle index is a measure of patch shape calculated as BPCRI = 1 − ($a_i/a_{c,i}$), where a_i is the area of the burnt patch *i* (m^2); and, $a_{c,i}$ equals the area of smallest circumscribing circle around the burnt patch *i* (m^2).
x	x	x	BPPAR	Burnt patch perimeter-area ratio is a measure of shape complexity calculated as BPPAR = p_i/a_i where pi is the perimeter of the burnt patch (meters) and a_i its area (sq. meters)
x		x	BPPRI	Burnt patch proximity index is a measure of isolation of burnt patches spatial distribution; it is calculated as $\Sigma(a_j/d_{ij}^2)$; it equals the sum of patch area, a_j (in m^2) divided by the distance squared, d_{ij}^2 (in m^2), between the focal burnt patch (i) and all neighboring burnt patches (j = 1,…,s) within a 1500 m radius
	x		DBRPE	Distance to burnt patch edge from each focal cell (meters)
Fire history and recent trends in burnt area				
x	x	x	MNBRA_90-04	Mean burnt area between 1990 and 2004
x	x	x	BRATR_90-04	Burnt area trend slope between 1990 and 2004
x	x	x	BRATR_95-04	Burnt area trend slope between 1995 and 2004
x	x	x	TBA2010_1000	Total burnt area in year 2010 considering a 1000 m buffer around recovering sites
x	x	x	TBA2011_1000	Total burnt area in year 2011 considering a 1000 m buffer around recovering sites

minimize remaining errors and noise in a two-step blind rejection approach for data cleaning and smoothing, following Marcos et al. (2012). First, to remove spurious values, we employed a filter based on the Hampel identifier (Hampel, 1974). Considered rather effective (Pearson, 2002), this method uses the concept of breakdown points based on local estimations of the median absolute deviation (MAD) and replaces the identified outliers with a local median. Then we used a *Savitzky-Golay* filter (Vaughan, 1982), which has been increasingly applied for cleaning, smoothing and reconstruction of NDVI time-series (Heumann et al., 2007; Nardini et al., 2004). All these computations were performed using the R programming environment, version 3.3.0 (R Development Core Team, 2016).

As post-fire recovery can develop in different phases and involving different processes (Bartels et al., 2016), we computed three indicators of post-fire recovery for the set of previously selected burnt pixels, using the NDVI time-series for the focal post-fire period (2006–2011):

(i) Half Recovery Time (HRT), a measure of short-term recovery velocity. HRT corresponds to the number of days necessary to reach the 50% level of recovery from the minimum NDVI value observed during the year of fire (i.e. 2005) to the pre-fire median (for years 2001–2004). According to Bartels et al. (2016), an indicator such as this one may give an approximation of the amount of time needed for a transition between a phase of rapid initial regeneration (in the first ca. 3 years after disturbance) to a more gradual one. This indicator was obtained through non-linear model fitting of the post-fire (i.e. 2006–2010) NDVI anomalies (to the "Gorgeous Year"), building on the approach described in Gouveia et al. (2010) and Bastos et al. (2011). We used the median as it is more robust against outliers and spurious values frequently found in NDVI time-series. HRT values below 100 days were excluded since these were considered less consistent with the distribution of remaining values in the area (as well as with those obtained by Gouveia et al. (2010)), also allowing to improve the performance and robustness of predictive models.

(ii) Recovery Trend Index (RTI), a measure of the recovery steepness, especially after the initial phase of rapid regrowth. It was computed as the slope of the trend in the NDVI data for the post-fire period using the Theil-Sen's estimator, a rank-based test that is robust against non-normality of the distribution and missing values (Theil, 1950). We used the R package *zyp* (Bronaugh et al., 2009), which accounts for inter-annual autocorrelation present in the data.

(iii) Cumulative Relative Recovery Index (CRRI), proposed for the first time in this study. CRRI is a more integrative measure of recovery, reflecting a longer period after the fire event, when the establishment of seedlings is usually successful (Bartels et al., 2016). It was calculated as the average of the yearly median relative recovery values in the post-fire period:

$$CRRI = \frac{1}{N}\sum_{i=1}^{N}\frac{|\widetilde{NDVI}_{post,i} - minNDVI_{fire}|}{\widetilde{NDVI}_{pre}}$$

where $\widetilde{NDVI}_{post,i}$ is the median NDVI of the year *i*, $minNDVI_{fire}$ is the minimum NDVI value during the year of fire, $\widetilde{NDVI}_{pre}$ is the median NDVI during the pre-fire period, and *N* is the number of years in the post-fire period (in this case *N* = 5 corresponding to 2006–2010).

2.4. Computation and pre-selection of predictive variables

In total, 236 predictive variables (see the complete list in Supplementary Material), organized in six groups, were considered in the initial dataset. To increase model parsimony, improve computation speed and reduce correlation/multicollinearity between predictors, we used the Random Forest variable importance features for conducting variable pre-selection using a three-stage algorithm. First, we ran 1000 RF replicates by predictor group (using default model settings) with 5% (randomly selected) of the initial dataset for calibration, and calculated variable importance statistics. For each round, the top ten variables with an absolute pairwise Spearman correlation below 0.8 were kept. We then quantified the frequency each selected variable entered the top ten and kept only the best five variables for each predictor group with a pairwise correlation below 0.7. Finally, we calculated the Spearman correlation matrix between all previously selected variables, within and across groups, and eliminated predictors with the lowest RF performance score from pairs recording an absolute correlation higher than 0.7.

As a result of this pre-selection algorithm, a total of 42 individual predictor variables were pre-selected for all response variables (Tables 1–3), 26 of which were used for modelling HRT, 25 for RTI, and 27 for CRRI. These variables, belonging to the six groups, are briefly described in the following paragraphs.

2.4.1. Fire traits

Fire severity and the spatial configuration of burnt areas have been shown to affect post-fire recovery (Bastos et al., 2011; Ireland and Petropoulos, 2015; Lee et al., 2014; Meng et al., 2015). To assess the predictive importance of these factors, we quantified fire severity by calculating the NDVI post-fire Break Magnitude Index (hereafter

Table 2
List of selected variables related to Environmental and physical attributes and to Post-fire climatic conditions from 2005 to 2007. Columns in the left display if the variable entered the final RF model for Cumulative Relative Recovery Index (CRRI), Recovery Trend Index (RTI) and Half Recovery Time (HRT).

CRRI	RTI	HRT	Variable acronym	Description
Environmental and physical attributes				
		x	BIO_02	Mean Diurnal Range calculated as mean of monthly maximum temperature – mean of monthly minimum temperature (°C)
x	x		BIO_07	Temperature Annual Range calculated as maximum temperature of the hottest month – minimum temperature of the coldest month (°C)
	x	x	BIO_15	Precipitation Seasonality calculated as the Coefficient of Variation of monthly total precipitation (mm)
	x	x	BIO_19	Precipitation of Coldest Quarter (mm)
x			MELEV	Mean elevation (meters a.s.l.)
x	x	x	PSLOP	Slope (%)
x		x	TOWEI	Topographic Wetness Index which is a steady state wetness index correlated with several soil attributes such as horizon depth, silt percentage, organic matter content
x	x		MRKTY	Main/dominant rock type
Post-fire climatic conditions (2005 to 2007)				
	x	x	TOTALPP_2005	Total precipitation for year 2005 (mm·year^{-1})
x			TOTALPP_2006	Total precipitation for year 2006 (mm·year^{-1})
x	x	x	TOTALPP_2007	Total precipitation for year 2007 (mm·year^{-1})
x			MAXTP_2006	Maximum temperature of the hottest month for 2006 (°C)
	x	x	MAXTP_2007	Maximum temperature of the hottest month for 2007 (°C)
x	x	x	MINTP_2007	Minimum temperature of the coldest month for 2007 (°C)

BRMGI), defined as the difference between the median NDVI for 2001–2004 (used as the pre-fire referential) and the 2005 minimum NDVI (Table 1). This indicator is a straightforward measure of the impact (severity) of fire on vegetation greenness, and it is similar to other measures already used in literature (e.g., White et al., 2017). A set of spatial pattern metrics were also computed to capture the spatial configuration and distribution of the previously selected burnt areas (see Table 1 and Supplementary Material) using ArcGIS and Fragstats (McGarigal et al., 2012).

2.4.2. Fire history and trends

Fire regime characteristics related to fire frequency are known to affect ecosystem resilience and hence the ability to recover to the pre-disturbance state (e.g., Díaz-Delgado et al., 2002). In order to evaluate these effects, historical fire recurrence, area and recent trends in burnt area prior to the focal year (2005) were calculated. (Table 1). These fire history variables were calculated considering three nested periods: 1990–2004, 1995–2004, and, 2000–2004, using the Portuguese National Cartographic Map of Burnt Areas (ICNF, 2016). Total burned area after 2005 (i.e., in the period from 2006 to 2011) around re-covering sites (within a buffer of 1000 m) was also calculated to portray the proximal effect of wildfires on recovery processes (Table 1).

2.4.3. Environmental/physical attributes

Topography, soils, lithology and pre-fire climatic regime play an important role in determining ecosystem response to wildfires and post-fire vegetation assembly (e.g., Díaz-Delgado et al., 2002, Meng et al., 2015, Shryock et al., 2015). We computed a set of variables describing the main environmental and physical attributes of the study area, such as geology/lithology, soil type, topography, hydrography, and pre-fire climate (Table 2). Average climatic conditions for pre-fire (1960–1990) were available from the *WorldClim* dataset (Hijmans et al., 2005). Geological and soil variables were based on the Portuguese Environmental Atlas (APA, 2013), and topographic features were calculated from the *ASTER GDEM* version 2 elevation dataset (Tachikawa et al., 2011).

Table 3
List of selected variables related to Landscape composition and to Pre-fire ecosystem functioning attributes. Columns in the left display if the variable entered the final RF model for Cumulative Relative Recovery Index (CRRI), Recovery Trend Index (RTI) and Half Recovery Time (HRT).

CRRI	RTI	HRT	Variable acronym	Description
Landscape composition				
x			PCLC2_750	% cover of agricultural areas in a 750 m buffer around the focal grid cell
	x		PCLC4	% cover of coniferous forest
		x	PCLC4_750	% cover of coniferous forest in a 750 m buffer around the focal grid cell
	x		PCLC4_1500	% cover of coniferous forest in a 1500 m buffer around the focal grid cell
		x	PCLC4_5000	% cover of coniferous forest in a 5000 m buffer around the focal grid cell
	x	x	PCLC5_5000	% cover of mixed forest in a 5000 m buffer around the focal grid cell
x			PCLC6_750	% cover of scrub and/or herbaceous vegetation associations in a 750 m buffer around the focal grid cell
x	x	x	PCLC6_5000	% cover of scrub and/or herbaceous vegetation associations in a 5000 m buffer around the focal grid cell
x			RDENS_1000	Density of roads in a 1000 m buffer around the focal grid cell (m/km^2)
Pre-fire ecosystem functioning attributes				
x	x		TIMAX_MN_5000	Time of NDVI maximum during a year – mean value in a 5000 m buffer around the focal grid cell (in days)
		x	TIMAX_SD_750	Time of NDVI maximum during a year – standard-deviation value in a 750 m buffer around the focal grid cell (in days)
x		x	TIMAX_SD_5000	Time of NDVI maximum during a year – standard-deviation value in a 5000 m buffer around the focal grid cell (in days)
		x	TIMXS_MN_750	*"Springness"* transformation of Time of maximum – mean value in 750 m buffer of the focal grid cell; "*Springness*" equals: (*sine*(TIMAX – 36)/23) × (2π) × (360/365), with TIMAX being the time of maximum
	x	x	TIMXS_MN_5000	*"Springness"* transformation of Time of maximum – mean value in 5000 m buffer of the focal grid cell
		x	TIMXW	*"Winterness"* transformation of Time of maximum; *"Winterness"* equals: (*cosine*(TIMAX – 36)/23) × (2π) × (360/365), with TIMAX being the time of maximum
	x		TIMXW_MN_750	*"Winterness"* transformation of Time of maximum – mean value in 750 m buffer of the focal grid cell
	x		LEGRS_MN_5000	Length of the growing season calculated as | TIMAX – TIMIN | (in days) – mean value in a 5000 m buffer around the focal grid cell; TIMAX and TIMIN are respectively the time of NDVI maximum and the time of minimum during a year
x			NTRSL_01_04	NDVI 2001–2004 trend slope (calculated through the Theil-Sen estimator)

2.4.4. Post-fire climatic conditions

Rainfall and temperature conditions following wildfires have been shown to determine the post-fire responses of vegetation (e.g., Díaz-Delgado et al., 2002; Meng et al., 2015; Shryock et al., 2015). Thus, a set of annual climatic variables related to temperature and precipitation for year 2005 (the focal fire year) and the closest post-fire years of 2006 and 2007 (Table 2) were calculated from climatic data available from the National Information System on Hydrological Resources (SNIRH) and the Portuguese Meteorological Institute (IPMA). Spatial interpolation, using Ordinary Kriging (implemented in R *gstat* package), was applied to obtain a complete coverage for the study area. For determining the best Kriging parameters, we ran and compared the predictive performance of different values for the nugget and range components of the semi-variogram while the partial-sill was kept fixed (equal to variance). Four model types were tested/compared: *Exponential*, *Spherical*, *Gaussian* and *Matern* as well as two model estimation types: Ordinary Least Squares (OLS) and Restricted Maximum Likelihood (REML). Then, for each climatic variable, 10-fold cross-validation was used to assess which parameter combination maximized predictive performance evaluated by the test R^2 (see also: https://github.com/joaofgoncalves/ClimKrig for more details on tested parameters). From this combination, we performed the interpolation for obtaining a continuous surface for the entire study area.

2.4.5. Landscape composition

Landscape heterogeneity and composition have also been found to influence post-fire vegetation density and regeneration (e.g., Bastos et al., 2011; Lee et al., 2014). To assess these effects, we quantified the composition of landscape mosaics for each 250 × 250 m grid cell and its surrounding area (Table 3). We used the Corine Land Cover for mainland Portugal (year 2000) to represent pre-fire conditions (Caetano et al., 2005, 2009) and calculated the percentage cover of eight broad land cover/use classes for each cell (see Supplementary Material). Additionally, to consider neighbourhood effects on vegetation recovery processes, we calculated the percentage cover of those same eight classes using three different buffer distances (750 m, 1500 m and 5000 m) around each recovering grid cell.

2.4.6. Pre-fire attributes of ecosystem functioning

Pre-fire ecosystem functioning attributes (EFAs), such as those related to productivity, seasonality, phenology and greenness, were used to capture several facets of pre-fire vegetation dynamics and heterogeneity (Table 3). These variables were calculated from annual NDVI time-series for the available pre-fire interval (from 2001 to 2004). For productivity (mainly related to vegetation amount and greenness), the mean and median values, as well as the maximum and minimum values for each year, were computed. For seasonality (intra-annual variation in vegetation amount and greenness), we calculated the range, the standard-deviation, the median absolute deviation, the coefficient of variation, a non-parametric coefficient of variation (i.e. the median absolute deviation divided by the median), the relative range (i.e. the difference between the maximum and minimum values, divided by the mean), and the non-parametric relative range (i.e. the difference between the maximum and minimum values, divided by the median). Finally, for phenology (timing in days of growing-season events), we calculated the moment (i.e. the 16-day maximum value composite) in which the maximum and the minimum values of each year occurred, as well as the difference between those two values, as an indicator of the length of the growing season. Furthermore, we applied transformations (such as the base-10 logarithm and the negative base-10 logarithm) to some of the seasonality-related variables. We also computed the "*springness*" and "*winterness*" of the phenological variables (Table 3), by transforming the original variables into polar coordinates and characterizing them by their sine and cosine values, respectively, in order to keep the continuous nature of consecutive annual periods (Alcaraz et al., 2006). We calculated the inter-annual median value for this period for all the above EFAs. In addition, similarly to landscape composition variables, we also incorporated neighbouring effects by calculating the mean and the standard deviation for each EFA at three different buffer distances: 750 m, 1500 m and 5000 m.

2.5. Model calibration and evaluation

To investigate and rank the drivers of post-fire recovery, we linked response variables (or post-fire indicators) to candidate predictors (Tables 1–3) with the Random Forest (RF) modelling algorithm (Breiman, 2001), implemented in the R *randomForest* package (Tang et al., 2004). The RF algorithm has shown excellent performance in high-dimensionality situations, due to its ability to handle complex interaction structures as well as highly correlated variables (Janitza, 2012; Oppel et al., 2009). Along with these features, it also provides measures of variable importance.

For RF parameterization, we used a *ntree* value (number of trees to grow) equal to 120, and the remaining parameters were set to default. In order to assess model performance, we used Monte Carlo cross-validation – MCCV (Xu et al., 2004), with 50%/50% train/test splits of the dataset (n = 20650 pixels/observations). A total of 100 different random splits/evaluation rounds were used in MCCV to estimate performance measures. Complementarily, we also used 10-fold cross-validation for performance evaluation. All results, including model predictions, performance statistics and variable importance measures, were then averaged across rounds. Regarding performance measures between observed and predicted values for the test sets, we used R^2, root-mean-square error (RMSE) and the normalized root-mean-square error (NRMSE).

2.6. Importance of individual predictors

Function *importance*, implemented in the *randomForest* package, was used to evaluate the importance of individual predictive variables, computed as the total decrease in node impurities from splitting each variable, averaged over all trees. For regression, node impurity is measured by the residual sum of squares. We set the *scale* parameter equal to *FALSE*, as suggested in Strobl and Zeileis (2008). Overall, the variable importance assessment focused on the relative ranking of variables instead of an absolute contribution to predictive accuracy.

3. Results

3.1. Post-fire recovery indicators

Large variations were observed for the three post-fire recovery indicators across the focal burnt areas, as illustrated in Fig. 3 for selected pixels. Spearman correlation (ρ) values for pairs of indicators where: $\rho = -0.35$ ($p < 0.0001$) between CRRI and RTI; $\rho = -0.10$ ($p < 0.0001$) between CRRI and HRT; and $\rho = 0.60$ ($p < 0.0001$) between RTI and HRT.

The three recovery metrics were variously influenced by fire severity and by the size of burnt area (Fig. 4). Higher values of the Break Magnitude Index (BRMGI; a proxy of fire severity) corresponded to lower values of RTI and CRRI, whereas only a small effect was observed for HRT (Fig. 4a). Regarding the size of burnt area (Fig. 4b), small-sized fires were predominantly associated with lower recovery values (especially for RTI and CRRI). Small fires were also characterized by higher fire severity (median values: $BRMGI_{< 50hectares} = 0.75$, $BRMGI_{\geq 50hectares} = 0.58$; Spearman correlation between burnt patch area and BRMGI: $\rho = -0.48$, $p < 0.0001$).

Post-fire recovery was also influenced by pre-fire land cover/vegetation type (Figs. 5 and 6). Most (86%) of the focal burnt areas corresponded to scrublands (47.10%), coniferous forests (17.50%), mixed coniferous-broadleaf forests (11.74%) or broadleaf forests (9.27%). Coniferous forests recorded much higher HRT median values (i.e.,

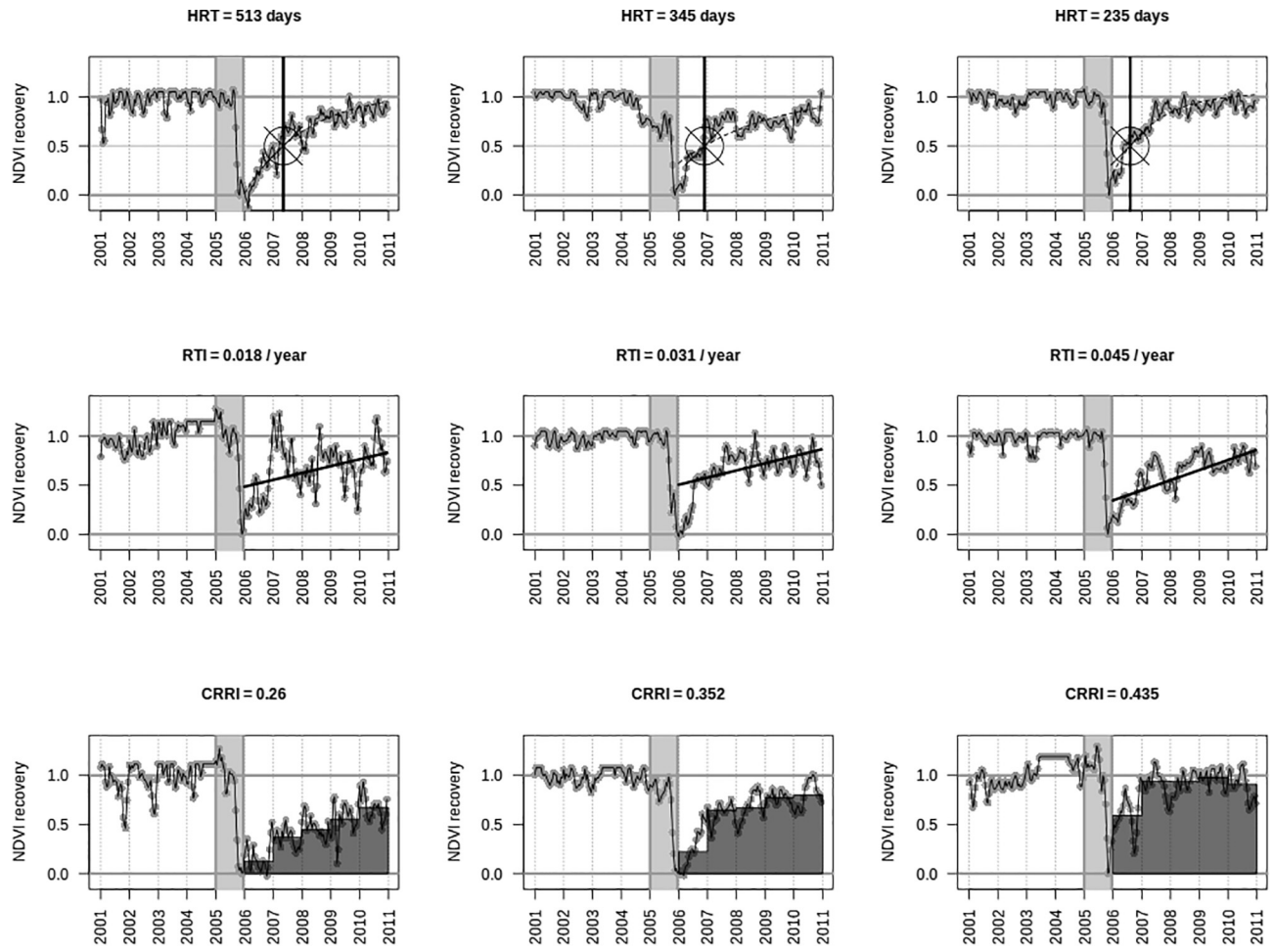

Fig. 3. Temporal profiles of the NDVI anomalies for burnt pixels (in year 2005) corresponding to low (left column), intermediate (middle column), and high recovery (right column) of each of the metrics of post-fire vegetation recovery used in this study: Half Recovery Time – HRT (top row), Recovery Trend Index – RTI (middle row) and Cumulative Relative Recovery Index – CRRI (bottom row).

slower initial recovery; Fig. 5a) but higher RTI (overall steeper recovery trend; Figs. 5b and 6). Smaller differences were observed for CRRI, with higher values recorded for scrublands, followed by broadleaf forests (Fig. 5c).

3.2. Model performance and determinants of post-fire recovery

The evaluation of *RF* models based on cross-validation test datasets showed a good performance for CRRI and RTI, while models for HRT yielded a moderate performance (Table 4).

Variables describing fire events (Fire traits group – FT), and particularly the BRMGI, were the most important factors to explain the observed variation in CRRI and RTI. The importance of BRMGI strongly decayed from CRRI to RTI (and more so to HRT; Table 5; Figs. 4a and 7). Overall, the fire history (FH) group of variables obtained the lowest predictive importance (Fig. 7).

For CRRI, the FT group of predictor variables ranked first (most importantly fire severity, expressed by BRMGI), whereas the remaining groups showed much less predictive importance (Fig. 7). For RTI, fire severity and burn patch perimeter-area ratio (both in the FT group) and post-fire climatic conditions (CC; total precipitation for the year 2005) ranked higher in terms of explanatory importance. To a less extent, landscape composition (LC; fraction cover of coniferous forest), pre-fire vegetation conditions linked to phenology (PC; "*winterness*" transformation of time of annual NDVI maximum) and geology (PA; dominant rock type) also played a role in explaining RTI (Fig. 7, Table 5).

For HRT, in contrast to the previous indicators, features related to landscape composition attained the highest predictive importance (Table 5, Fig. 7). Differences in HRT were found for distinct vegetation types (Fig. 5) with coniferous forests recording the highest values (synonymous of slower recovery). The fraction cover of mixed coniferous/broadleaf forests or scrublands also recorded relatively higher predictive importance (Table 5). In addition, post-fire climatic conditions (minimum temperature of the coldest month for 2007), average climatic regime (temperature mean diurnal range) and fire severity (BRMGI) also scored higher importance (Table 5, Fig. 7).

4. Discussion and conclusions

4.1. Satellite remote sensing of post-fire recovery

Remote sensing has received increasing attention in fire ecology, not only to detect wildfires but also to assess how ecosystems respond to those disturbance events (e.g., Chuvieco et al., 2010; Di-Mauro et al., 2014; Gouveia et al., 2010; Lentile et al., 2006). To analyse the spatiotemporal patterns of post-fire vegetation recovery, we developed and tested three candidate indicators based on MODIS NDVI time-series: the Half Recovery Time (HRT), the Recovery Trend Index (RTI), and the Cumulative Relative Recovery Index (CRRI). Moreover, random forests (RF) models revealed clear differences in the effects of multiple predictors (and groups of predictors) on the three post-fire recovery indicators.

The Half Recovery Time (HRT) is a non-linear measure of the short-term recovery rate that corresponds to the number of days necessary to

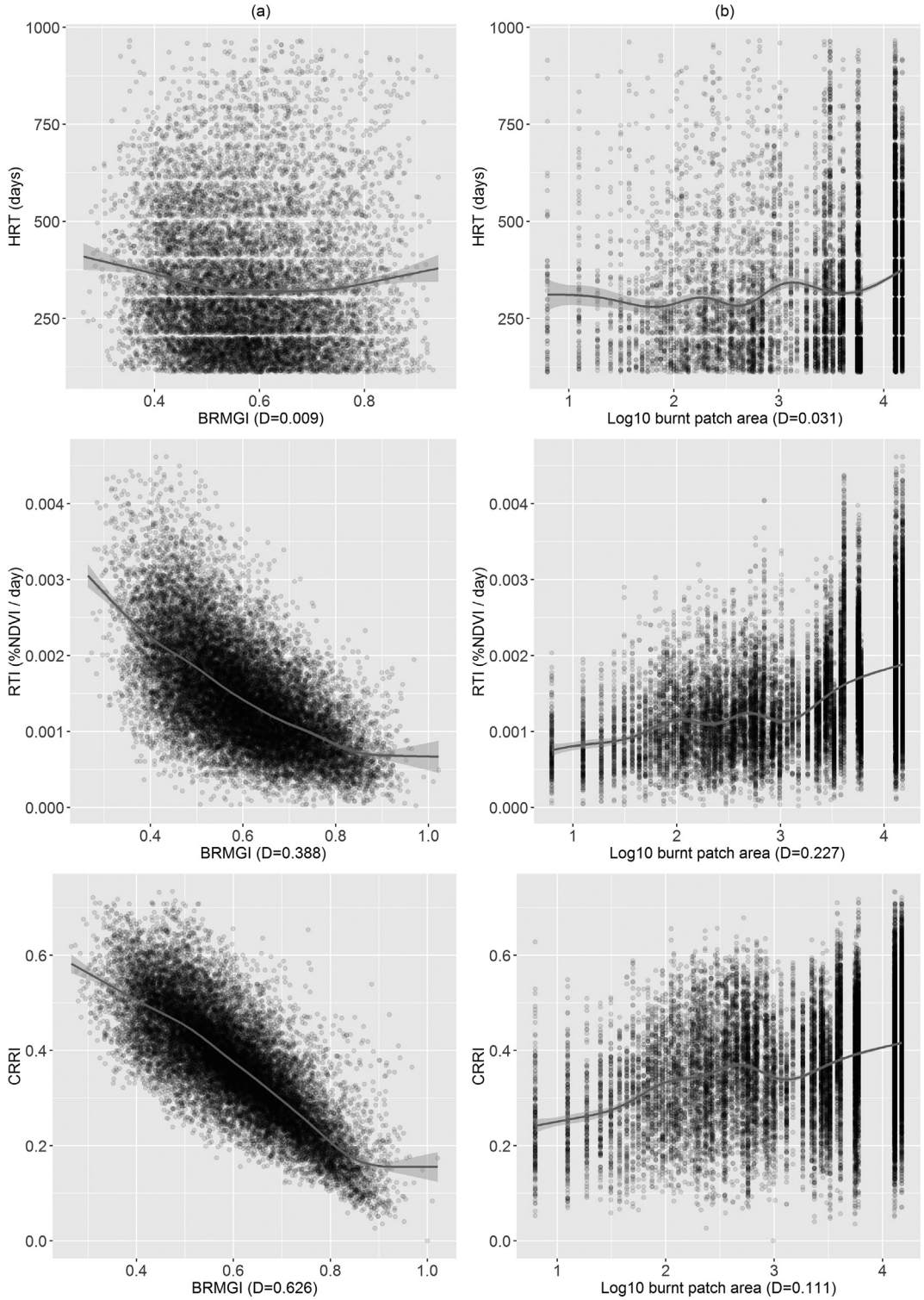

Fig. 4. Biplots showing the association between BRMGI (break magnitude index, a proxy for fire severity) and (a) recovery indicators and (b) Log10-transformed burnt patch area. The blue line represents a non-linear semi-parametric GAM smooth. The 'D' in the xx-axis label represents the explained deviance by the smooth curve.

reach the 50% level of pre-fire conditions (set as the 2001–2004 median). For this indicator, the structural features of the landscape (composition and spatial configuration) at focal and contextual levels, as well as post-fire climatic conditions, were identified as the most important factors. The effects of landscape structure at different distances around the focal burnt areas (see Table 5) highlight the importance of a multi-scalar approach to analyse the effects of landscape structure on fire occurrence and on post-fire recovery (Lozano et al., 2010; Morgan et al., 2001). It also reveals the importance of considering landscape heterogeneity in the assessment of fire regimes and post-fire recovery processes.

The Recovery Trend Index (RTI) is a linear measure of recovery steepness, computed as the slope of the trend in the NDVI data for the post-fire period. For this indicator, BRMGI was the variable recording the highest predictive importance (as well as for CRRI; see Table 5). This variable translates the relative decrease in NDVI produced by the

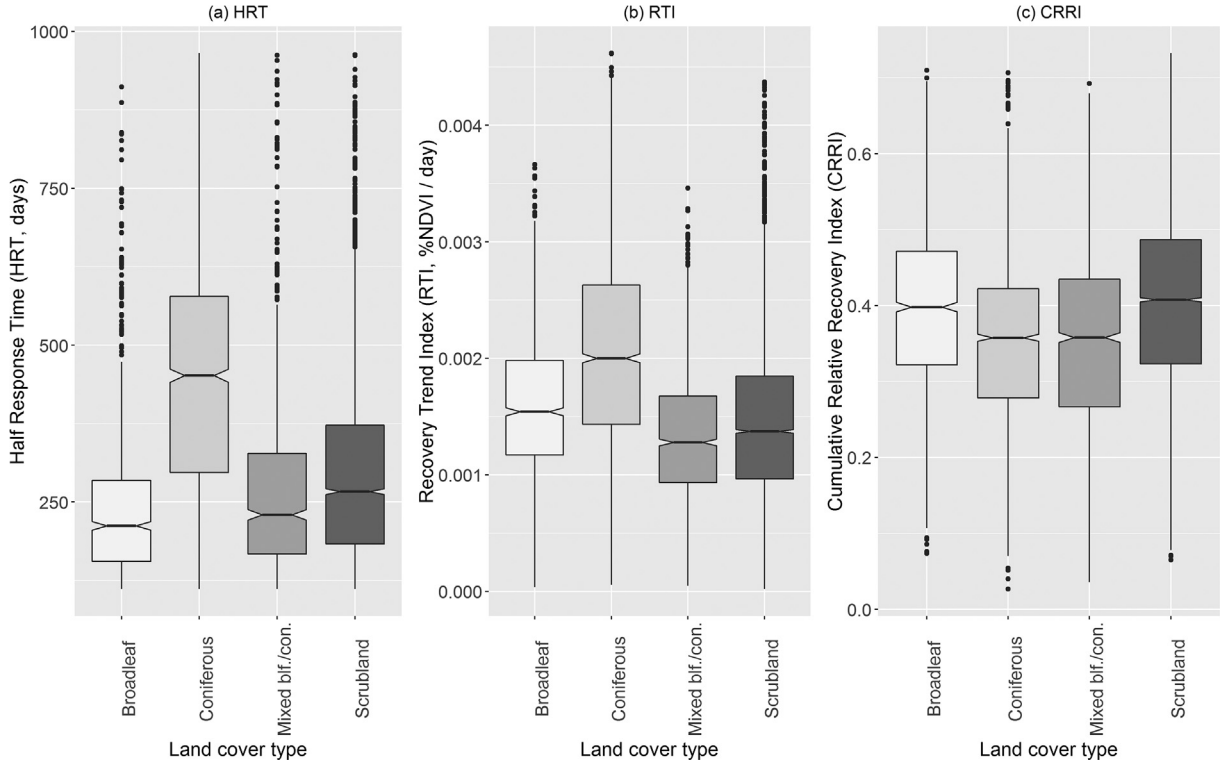

Fig. 5. Boxplots displaying differences in the distribution of the (a) Half Response Time (HRT), (b) Recovery Trend Index (RTI) and (c) Cumulative Relative Recovery Index (CRRI) for pixels with four different dominant land cover/vegetation types (occupying > 95% of the pixel). Outliers (i.e., points ± 1.5 times the interquartile distance), are represented as points.

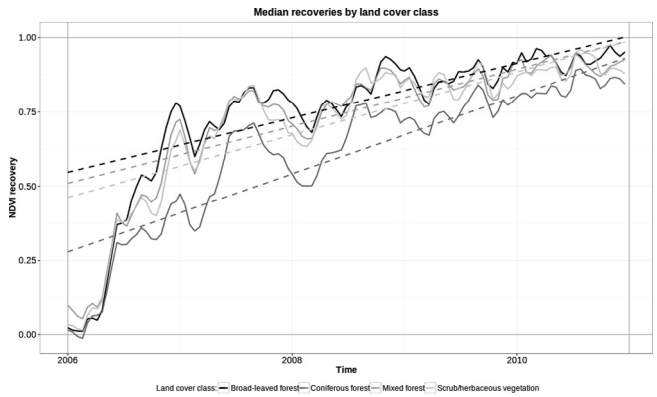

Fig. 6. Median recovery profiles for different land cover/vegetation types. The estimated prewhitened linear trend coefficients were: broad-leaved forest = 3.99×10^{-4}, coniferous forest = 5.72×10^{-4}, mixed forest = 4.18×10^{-4}, and scrub/herbaceous vegetation = 4.59×10^{-4}. 'Coniferous forest' land cover type recorded the highest trend slope consistent with RTI values.

Table 4
Random Forest model performance for the test set, based on R^2, root-mean-square error (RMSE), and normalized root-mean-square error (NRMSE).

Model (response variable)	R^2	RMSE	NRMSE
CRRI	0.85	4.47×10^{-2}	5.08
RTI	0.77	3.38×10^{-4}	4.81
HRT	0.52	124	14.5

fire event in regard to the pre-fire NDVI mean (2001–2004). It is thus a proxy for the severity of the fire event (see Fig. 3). There is a well-known relation between fire severity and post-fire recovery, with more severe fires causing a higher depletion of the recovery capacity of burnt areas whereas less severe fires are often followed by rapid recovery (Díaz-Delgado et al., 2002; Van Leeuwen et al., 2010). Lee et al. (2014) found that, together with the compositional and spatial heterogeneity of pre-fire forest, burn severity had a significant impact on post-fire vegetation density and regeneration. Ireland and Petropoulos (2015) also found a negative correlation between fire damage and recovery. Nevertheless, we found that the predictive importance of BRMGI decays considerably from CRRI and HRT to HRT (see Figs. 4 and 7). This suggests that fire severity expresses its effect over a longer period of time, whereas in a shorter time span landscape composition (namely the dominant forest type) played a more important role.

For RTI, the features of the fire event and the post-fire climatic conditions were the more important predictive factors. Although with lower predictive importance, landscape composition and pre-fire conditions (mostly related to vegetation phenology; Table 5 and Fig. 7) also explained some of the RTI variation. The recovery process as portrayed by this indicator thus seems to respond to a complex interaction of functional and structural constraints. An example of structural effects is the BPPAR variable (i.e., burnt patch perimeter-area ratio, negatively correlated to burnt patch area, $\rho = -0.89$, $p < 0.0001$). This variable had a relatively high predictive importance for RTI (and for CRRI, to a lesser extent; see Table 5). This partially expresses an indirect relation with burnt severity since burnt patches with lower BPPAR (i.e., with larger area) usually hold higher spatial heterogeneity and thus higher internal variability in burnt severity (Lee et al., 2014). This heterogeneity potentially allows the occurrence of less impacted or even unburned 'islands' (Román-Cuesta et al., 2009). Mixed-severity fires often create heterogeneous landscape mosaics due to the variation in recovery rates and recruitment conditions (Hayes and Robeson, 2011). Thus, a more direct effect on recovery could also emerge in larger areas (with higher heterogeneity of burn severity) since less severely burned or unburned 'islands' can act as seed sources that may enhance post-fire vegetation regeneration (Ordóñez et al., 2005; Román-Cuesta et al., 2009; Turner and Romme, 1994).

Finally, the Cumulative Relative Recovery Index (CRRI), proposed in this study, is a measure of the extent of recovery, calculated as the average of the yearly median relative recovery values in the post-fire

Table 5
Ranking of the relative contribution of predictive variables (and groups of variables) for models calibrated for each response variable (i.e. post-fire recovery indicator): Half Recovery Time (HRT), Recovery Trend Index (RTI) and, Cumulative Relative Recovery Index (CRRI). Only the top 10 variables are shown. Groups of explanatory variables: FT (Fire Traits); PC (Pre-fire conditions/EFAs); LC (Landscape composition); PA (Environmental/physical attributes), CC (Post-fire climatic conditions) and FH (Fire history). Relative importance (RI) calculated as: $RI = [I_i/\max(I_i)] \times 100$, with I_i equal to the importance of variable i as determined by the Random Forest algorithm.

Resp. var.	Rank	Rel. importance (%)	Group	Variable acronym	Variable description
HRT	**#1**	100.0	**LC**	PCLC4_750	% cover of Coniferous forest in a 750 m buffer
	#2	61.3	LC	PCLC4_5000	% cover of Coniferous forest in a 5000 m buffer
	#3	48.4	**CC**	MINTP_2007	Minimum temperature of the coldest month for 2007
	#4	46.8	LC	PCLC5_5000	% cover of Mixed forest in a 5000 m buffer
	#5	46.1	**PA**	BIO02	Temperature Mean Diurnal Range
	#6	43.4	**FT**	BRGMI	NDVI post-fire break magnitude index
	#7	43.2	PA	BIO19	Precipitation of Coldest Quarter
	#8	42.5	CC	TOTALPP_2005	Total precipitation for year 2005
	#9	40.1	LC	PCLC6_5000	% cover of Scrub and/or herbaceous vegetation associations in a 5000 m buffer
	#10	37.4	PA	BIO15	Precipitation Seasonality
RTI	**#1**	100.0	**FT**	BRGMI	NDVI post-fire break magnitude index
	#2	38.4	FT	BPPAR	Burnt patch perimeter-area ratio
	#3	26.3	**CC**	TOTALPP_2005	Total precipitation for year 2005
	#4	20.9	**LC**	PCLC4_1500	% cover of Coniferous forest in a 1500 m buffer
	#5	17.5	**PC**	TIMXW_MN_750	"*Winterness*" transformation of Time of maximum – mean value in 750 m buffer of the focal grid cell
	#6	15.9	LC	CLC4	% cover of Coniferous forest
	#7	14.6	FT	DBRPE	Distance to burnt patch edge
	#8	14.5	PC	TIMXS_MN_5000	"*Springness*" transformation of Time of maximum – mean value in 5000 m buffer of the focal grid cell
	#9	14.2	CC	TOTALPP_2007	Total precipitation for year 2007
	#10	12.5	**PA**	MRKTY	Main/dominant rock type
CRRI	**#1**	100.0	**FT**	BRGMI	NDVI post-fire break magnitude index
	#2	7.8	**PC**	NTRSL_01_04	NDVI 2001–2004 trend slope
	#3	7.4	FT	BPPAR	Burnt patch perimeter-area ratio
	#4	5.8	**PA**	MELEV	Mean elevation
	#5	5.0	**CC**	MAXTP_2006	Maximum temperature of the hottest month for 2006
	#6	4.9	**LC**	PCLC6_750	% cover of Scrub and/or herbaceous vegetation associations in a 750 m buffer
	#7	4.5	**FH**	MNBRA_90-04	Mean burnt area between 1990 and 2004
	#8	4.4	CC	TOTALPP_2007	Total precipitation for year 2007
	#9	4.2	CC	TOTALPP_2006	Total precipitation for year 2006
	#10	4.1	LC	PCLC2_750	% cover of Agricultural areas in a 750 m buffer

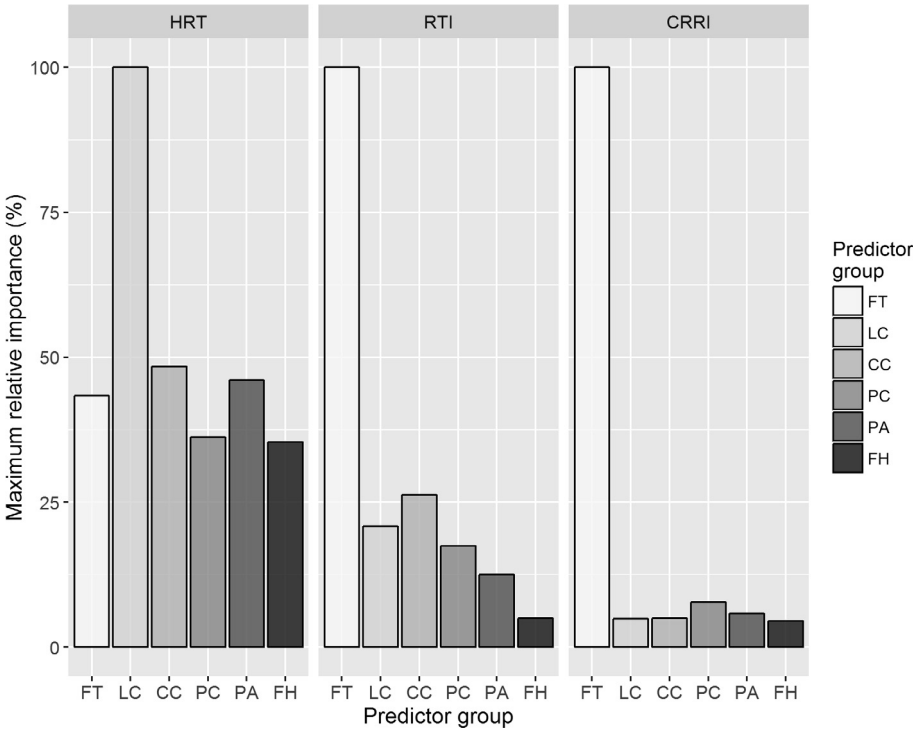

Fig. 7. Barplot showing the maximum value for Relative Importance (RI; calculated as $RI = [I_i/\max(I_i)] \times 100$, with I_i equal to the importance of variable i as determined by the Random Forest algorithm), per variable group for each response variable: Cumulative Relative Recovery Index (CRRI), Recovery Trend Index (RTI) and, Half Recovery Time (HRT). Groups of explanatory variables include: FT (Fire Traits); PC (Pre-fire conditions/EFAs); LC (Landscape composition); PA (Environmental/physical attributes); CC (Post-fire climatic conditions) and FH (Fire history). Variable importance values were estimated using Random Forest functions.

period. Again, the BRMGI was the variable recording the highest predictive importance for explaining CRRI (see Fig. 7). In addition, fires with smaller areas recorded the lowest values for CRRI (and RTI; see Fig. 4). Overall, the features of the fire event (e.g., fire severity, spatial patterning of burnt area) were the dominant constraints to explain the recovery process as portrayed by this indicator. Similarly, Martín-Alcón and Coll (2016) found that *Pinus nigra* has locally resilient responses driven by fire effects (presence of unburned patches and burn severity) and by the characteristics of the pre-fire vegetation (such as the presence of stable forest areas) that determine seed recruitment supplied by surviving individuals. To a much lesser extent, pre-fire conditions and post-fire climate also contributed to explain the spatial variation of this indicator (see Fig. 7).

These three indicators jointly allow an integrative assessment of the post-fire recovery process. Short-term recovery response, as assessed by the HRT indicator, was strongly linked to landscape composition and specifically to the percentage of coniferous forests, mixed coniferous/broadleaf forests, and scrublands (see Table 5). Typically, coniferous species recover from the seed bank and thus have slower recovery times in comparison to resprouting species (such as broadleaf and scrubland species), as observed here (see Figs. 5a and 6) and in previous studies (e.g.: Bastos et al., 2011; Pausas and Bradstock, 2007; Shatford et al., 2007; Shryock et al., 2015). Although the CRRI indicator recorded relatively less differentiation among land cover types (see Fig. 5c), coniferous forests also obtained the lowest recovery values for this indicator; however, in contrast, RTI values for coniferous forest species were the highest (see Fig. 5b). This seemingly contradictory result may be due to the fact that coniferous dominated areas have a slower recovery immediately after the fire (hence higher HRT), however their average trend in a longer timeframe is actually steeper (higher RTI), with similar median NDVI values observed across land cover classes towards the end of the analysed time-series (see Fig. 6).

4.2. Indicators and determinants of post-fire recovery

Overall, differences in the predictive importance of the several groups of variables allowed to describe and understand the responses of each of the recovery indicators, and to portray different facets of the post-fire vegetation recovery process. Three sets of predictive variables consistently obtained higher relative importance: (i) Fire traits (FT), especially BRMGI (characterizing fire severity) and BPPAR (burn patch perimeter-area ratio; linked to burnt severity heterogeneity); (ii) Landscape composition (LC) particularly the fraction cover of coniferous forests; and (iii) post-fire climatic conditions (CC), namely minimum and maximum temperatures and total precipitation.

The HRT, an indicator of short-term recovery, was clearly more related to the LC and CC groups. This indicator captured the half-recovery time (or speed), mainly related to differences in fire-recovery traits of vegetation, to climate conditions after the fire event, and to interactions between these and (to a lesser extent) other factors. The role of post-fire climatic conditions as an important predictor of recovery was described in previous studies (e.g., Meng et al., 2015; Shryock et al., 2015). Keeley et al. (2005) showed that scrubland recovery under Mediterranean climate in California is strongly determined by precipitation patterns, and Nelson et al. (2014) found that *Artemisia tridentata* recovery was positively linked to precipitation following the fire. Moreover, re-sprouting capacity is known to be positively related to precipitation following fire (DeFalco et al., 2010; Nano and Clarke, 2011; Pausas and Bradstock, 2007).

The RTI indicator, expressing mid-term recovery, was mainly driven by the FT and CC groups, but also, to a less extent, by the LC group. This indicator expresses the steepness of the linear trend at the mid-term recovery (or long-term, depending on the extension of the time-series). As such, RTI captures multiple interacting effects that shape the recovery process in terms of vegetation functioning. Since its computation is based on a rank-based method, it is robust against non-normality and missing values (Theil, 1950) and less influenced by seasonality and intra-annual peaks or fluctuations that occur during recovery. These features make RTI a promising indicator of mid-to-long term post-fire recovery under distinct climate regimes.

Finally, our long-term recovery indicator (CRRI) was strongly related to fire attributes (FT group; essentially the spatial variation of fire severity) and was much less driven by vegetation type and structure or by climatic conditions following the fire event. This indicator is influenced by intra-annual fluctuations since it is based on annual median values, thus capturing the entire time-series recovery integral on a yearly basis (similarly to Veraverbeke et al., 2011). By accounting for differences in pre-fire conditions (i.e., pre-fire median), it allows comparisons across sites. This indicator expresses post-fire recovery completeness related to ecosystem functioning (e.g., Van Leeuwen et al., 2010), in the mid-term or long-term depending on the extent of the time-series and on the specific (pyro-)environmental context.

Overall, our results for the three proposed indicators suggest that they can capture the interacting effects of the biotic processes (e.g., seed delivery or supply, competition, recovery capacity determined by species life-history traits) and abiotic filters (e.g., post-fire precipitation and temperature) that determine the early post-fire recovery process. In the mid-to-long term, recovery responses mainly link back to the depletion of resilience capacity and the amount of change impacting vegetation structure and functioning caused by differential fire severity. Over a longer temporal context, the effect of species traits and inter-annual variations in climate tend to be averaged out, thus having lower relative importance (see Johnstone et al., 2016).

4.3. Towards improved management of post-fire recovery and fire hazard

Our results suggest that the three recovery indicators express different aspects of the recovery process. Given their distinct definitions and computation, as well as their responses to different sets of determinants, they seem to cover different stages and facets of the post-fire recovery process. This supports the usefulness of multi-indicator functional approaches, based on high-temporal resolution remote sensing time-series of spectral vegetation indices, to fully analyse key ecosystem properties and processes (Alcaraz et al., 2006; Di-Mauro et al., 2014; Van Leeuwen et al., 2010). Our three indicators were not strongly correlated across a large, heterogeneous and heavily burnt region, jointly allowing a more integrative view of vegetation recovery, a key issue when evaluating ecosystem resilience (Lavorel, 1999; Moretti and Legg, 2009; Pausas and Lloret, 2007).

Post-fire recovery capacity is a key determinant of the rapid re-establishment of pre-fire ecosystem functioning and provision of ecosystem services (Bugalho et al., 2011; Duguy et al., 2012). At the same time, this recovery will also increase fuel biomass accumulation across the landscape (Lloret et al., 2002; Moreira et al., 2011), thus amplifying fire hazard and originating a trade-off challenge to authorities in charge of nature conservation and landscape management. Our results suggest that forest and landscape planning for improved post-fire recovery should consider the functional dimension of landscapes besides their structural attributes, especially when defining broad planning and management units. This adds to the several other applications of remote sensing tools in fire detection and in fire risk management (Chuvieco et al., 2010). In addition, besides mapping burned areas, national and/or regional authorities should also focus on mapping fire severity since this is a major driver of post-fire recovery. Our study illustrates how existing satellite platforms can be very useful in this regard. The resulting information could further be useful for prioritizing actions of fire impact mitigation and post-fire restoration. Given the importance of post-fire climatic conditions (precipitation and temperature) to explain recovery processes, monitoring these parameters, with as high spatial and temporal resolution data as possible, is also crucial to assess the rate of vegetation recovery.

Post-fire NDVI anomalies in the interannual mean and range of

photosynthetic activity were usually higher than during pre-fire conditions (see Fig. 3). This pattern was expected since NDVI is positively correlated to vegetation cover (De Keersmaecker et al., 2014), productivity (Jobbágy et al., 2014) and leaf area index (Carlson and Ripley, 1997; Wang et al., 2005). Moreover NDVI-based recovery indices showed a general pattern of fast recovery immediately after the fire and a non-linear gradual decrease in response speed (typically after 6–12 months), as observed by Ireland and Petropoulos (2015). Overall, this suggests a higher dependence of suitable environmental (namely climatic) conditions in early post-fire recovery, often related to the replacement of pre-fire vegetation by early successional vegetation types. Increased variance and 'flickering' has also been related to potential critical transitions in vegetation state and properties such as resilience (Dakos et al., 2013, 2012). The depletion of resilience to disturbances decreases the self-repairing capacity of ecosystems (Folke et al., 2004) and increases the risk of sudden regime shifts, posing a serious challenge to the management of natural capital (Boettiger et al., 2013).

In this study, we showed that a multi-indicator functional approach based on time series of remotely-sensed vegetation indices, combined with machine learning techniques, can be rather useful in post-fire research and management. The potential applications range from evaluating post-fire processes and rates to assessing their main driving factors, with benefits for landscape management and monitoring, post-fire ecosystem restoration, and risk governance. The continuous data streams coming from currently available satellite platforms (e.g., ESA/Copernicus Sentinel program) opens new opportunities to track post-fire dynamics from space, allowing managers and other stakeholders to make more informed and timely decisions.

Acknowledgments

João Torres, J. F. Gonçalves and B. Marcos were financially supported by FCT (Portuguese Foundation for Science and Technology), through PhD Grants SFRH/BD/24560/2005, SFRH/BD/90112/2012 and SFRH/BD/99469/2014, respectively, funded by National and European Funds (ESF), through POPH-QREN (2007-2013) and/or CSF (2014-2020). J.P. Honrado received support from the European Union's Horizon 2020 Research and Innovation Programme, under Grant Agreement No 641762 (ECOPOTENTIAL).

Appendix A. Supplementary data

Supplementary data associated with this article can be found, in the online version, at http://dx.doi.org/10.1016/j.ecolind.2018.02.008.

References

Alcaraz, D., Paruelo, J., Cabello, J., 2006. Identification of current ecosystem functional types in the Iberian Peninsula. Global Ecol. Biogeogr. 15, 200–212. http://dx.doi.org/10.1111/j.1466-822X.2006.00215.x.

Alcaraz-Segura, D., Cabello, J., Paruelo, J.M., Delibes, M., 2008. Trends in the surface vegetation dynamics of the national parks of Spain as observed by satellite sensors. Appl. Veg. Sci. 11, 431–440. http://dx.doi.org/10.3170/2008-7-18522.

Alcaraz-Segura, D., Lomba, A., Sousa-Silva, R., Nieto-Lugilde, D., Alves, P., Georges, D., Vicente, J.R., Honrado, J.P., 2017. Potential of satellite-derived ecosystem functional attributes to anticipate species range shifts. Int. J. Appl. Earth Obs. Geoinf. 57, 86–92. http://dx.doi.org/10.1016/j.jag.2016.12.009.

Angelis, A., Bajocco, S., Ricotta, C., de Angelis, A., Bajocco, S., Ricotta, C., 2012. Phenological variability drives the distribution of wildfires in Sardinia. Landscape Ecol. 27, 1535–1545. http://dx.doi.org/10.1007/s10980-012-9808-2.

APA, 2013. Atlas do Ambiente, Agência Portuguesado Ambiente, URL: http://sniamb.apambiente.pt/webatlas/index.html.

Bajocco, S., Ricotta, C., 2008. Evidence of selective burning in Sardinia (Italy): which land-cover classes do wildfires prefer? Landscape Ecol. 23, 241–248. http://dx.doi.org/10.1007/s10980-007-9176-5.

Bajocco, S., Rosati, L., Ricotta, C., 2010. Knowing fire incidence through fuel phenology: a remotely sensed approach. Ecol. Modell. 221, 59–66. http://dx.doi.org/10.1016/j.ecolmodel.2008.12.024.

Bartels, S.F., Chen, H.Y.H., Wulder, M.A., White, J.C., 2016. Trends in post-disturbance recovery rates of Canada's forests following wildfire and harvest. For. Ecol. Manage. 361, 194–207. http://dx.doi.org/10.1016/j.foreco.2015.11.015.

Bastos, A., Gouveia, C.M., Dacamara, C.C., Trigo, R.M., 2011. Modelling post-fire vegetation recovery in Portugal. Biogeosciences 8, 3593–3607. http://dx.doi.org/10.5194/bg-8-3593-2011.

Beven, K., Germann, P., 2013. Macropores and water flow in soils revisited. Water Resour. Res. 49, 3071–3092. http://dx.doi.org/10.1002/wrcr.20156.

Boettiger, C., Ross, N., Hastings, A., 2013. Early warning signals: the charted and uncharted territories. Theor. Ecol. 6, 255–264.

Breiman, L., 2001. Random forests. Mach. Learn. 45, 5–32. http://dx.doi.org/10.1023/A:1010933404324.

Bronaugh, D., Werner, A., Bronaugh, M.D., 2009. Package "zyp". CRAN Repos.

Bugalho, M.N., Caldeira, M.C., Pereira, J.S., Aronson, J., Pausas, J.G., 2011. Mediterranean cork oak savannas require human use to sustain biodiversity and ecosystem services. Front. Ecol. Environ. 9, 278–286. http://dx.doi.org/10.1890/100084.

Caetano, M., Mata, F., Freire, S., 2005. Accuracy assessment of the Portuguese CORINE Land Cover map. Glob. Dev. Environ. Earth Obs. 459–467.

Caetano, M., Nunes, V., Nunes, A., 2009. CORINE Land Cover 2006 for Continental Portugal 97.

Carlson, T.C., Ripley, D.A., 1997. On the relationship between NDVI, fractional vegetation cover, and leaf area index. Remote Sens. Environ. 62, 241–252.

Cavallero, L., López, D.R., Raffaele, E., Aizen, M.A., 2015. Structural–functional approach to identify post-disturbance recovery indicators in forests from northwestern Patagonia: a tool to prevent state transitions. Ecol. Indic. 52, 85–95. http://dx.doi.org/10.1016/j.ecolind.2014.11.019.

Chuvieco, E., Aguado, I., Yebra, M., Nieto, H., Salas, J., Martín, M.P., Vilar, L., Martínez, J., Martín, S., Ibarra, P., de la Riva, J., Baeza, J., Rodríguez, F., Molina, J.R., Herrera, M.A., Zamora, R., 2010. Development of a framework for fire risk assessment using remote sensing and geographic information system technologies. Ecol. Modell. 221, 46–58. http://dx.doi.org/10.1016/j.ecolmodel.2008.11.017.

Costa, J.C., Aguiar, C., Capelo, J.H., Lousã, M., Neto, C., 1998. Biogeografia de Portugal Continental. Quercetea 0, pp. 5–56. doi:citeulike-article-id:9981809.

Dakos, V., van Nes, E.H., D'Odorico, P., Scheffer, M., 2012. Robustness of variance and autocorrelation as indicators of critical slowing down. Ecology 93, 264–271. http://dx.doi.org/10.1890/11-0889.1.

Dakos, V., van Nes, E.H., Scheffer, M., 2013. Flickering as an early warning signal. Theor. Ecol. 6, 309–317. http://dx.doi.org/10.1007/s12080-013-0186-4.

De Keersmaecker, W., Lhermitte, S., Tits, L., Honnay, O., Somers, B., Coppin, P., 2014. Linking NDVI and climate-based ecosystem stability with land cover in Europe. In: 2014 IEEE Geoscience and Remote Sensing Symposium. IEEE, pp. 3938–3940. doi:10.1109/IGARSS.2014.6947346.

DeFalco, L.A., Esque, T.C., Scoles-Sciulla, S.J., Rodgers, J., 2010. Desert wildfire and severe drought diminish survivorship of the long-lived Joshua tree (Yucca brevifolia; Agavaceae). Am. J. Bot. 97, 243–250. http://dx.doi.org/10.3732/ajb.0900032.

Díaz-Delgado, R., Lloret, F., Pons, X., Terradas, J., 2002. Satellite evidence of decreasing resilience in mediterranean plant communities after recurrent wildfires. Ecology 83, 2293–2303. http://dx.doi.org/10.1890/0012-9658(2002).

Di-Mauro, B., Fava, F., Busetto, L., Crosta, G.F., Colombo, R., Di Mauro, B., Fava, F., Busetto, L., Crosta, G.F., Colombo, R., 2014. Post-fire resilience in the Alpine region estimated from MODIS satellite multispectral data. Int. J. Appl. Earth Obs. Geoinf. 32, 163–172. http://dx.doi.org/10.1016/j.jag.2014.04.010.

Duguy, B., Alloza, J.A., Baeza, M.J., De La Riva, J., Echeverría, M., Ibarra, P., Llovet, J., Cabello, F.P., Rovira, P., Vallejo, R.V., 2012. Modelling the ecological vulnerability to forest fires in mediterranean ecosystems using geographic information technologies. Environ. Manage. 50, 1012–1026. http://dx.doi.org/10.1007/s00267-012-9933-3.

EFFIS., 2015. http://effis.jrc.ec.europa.eu/.

European Commission, 2010. Forest Fires in Europe 2009. In: Publication Office of the European Union, EUR 24502 EN, pp. 83.

Folke, C., Carpenter, S., Walker, B., Scheffer, M., Elmqvist, T., Gunderson, L., Holling, C.S., 2004. Regime shifts, resilience, and biodiversity in ecosystem management. Annu. Rev. Ecol. Evol. Syst. 557–581.

Gouveia, C., DaCamara, C.C., Trigo, R.M., 2010. Post-fire vegetation recovery in Portugal based on spot/vegetation data. Nat. Hazard. Earth Syst. Sci. 10, 673–684. http://dx.doi.org/10.5194/nhess-10-673-2010.

Gumming, S.G., 2001. Forest type and wildfire in the Alberta boreal mixedwood: what do fires burn? Ecol. Appl. 11, 97–110. http://dx.doi.org/10.1890/1051-0761(2001)011[0097:FTAWIT]2.0.CO;2.

Hampel, F.R., 1974. The influence curve and its role in robust estimation. J. Am. Stat. Assoc. 69, 383–393. http://dx.doi.org/10.1080/01621459.1974.10482962.

Hayes, J.J., Robeson, S.M., 2011. Relationships between fire severity and post-fire landscape pattern following a large mixed-severity fire in the Valle Vidal, New Mexico. U.S.A. For. Ecol. Manage. 261, 1392–1400. http://dx.doi.org/10.1016/j.foreco.2011.01.023.

Helman, D., Lensky, I., Tessler, N., Osem, Y., 2015. A phenology-based method for monitoring woody and herbaceous vegetation in mediterranean forests from NDVI time series. Remote Sens. 7, 12314–12335. http://dx.doi.org/10.3390/rs70912314.

Heumann, B.W., Seaquist, J.W., Eklundh, L., Jönsson, P., 2007. AVHRR derived phenological change in the Sahel and Soudan, Africa, 1982–2005. Remote Sens. Environ. 108, 385–392. http://dx.doi.org/10.1016/j.rse.2006.11.025.

Hijmans, R.J., Cameron, S.E., Parra, J.L., Jones, P.G., Jarvis, A., 2005. Very high resolution interpolated climate surfaces for global land areas. Int. J. Climatol. 25, 1965–1978. http://dx.doi.org/10.1002/joc.1276.

ICNF, 2016. Cartografia nacional de áreas ardidas [WWW Document]. URL < http://www.icnf.pt/portal/florestas/dfci/inc/info-geo > .

Ireland, G., Petropoulos, G.P., 2015. Exploring the relationships between post-fire vegetation regeneration dynamics, topography and burn severity: a case study from the

Montane Cordillera ecozones of Western Canada. Appl. Geogr. 56, 232–248. http://dx.doi.org/10.1016/j.apgeog.2014.11.016.
Janitza, A.B.S., 2012. Overview of random forest methodology and practical guidance with emphasis on computational biology and overview of random forest methodology and practical guidance with emphasis on computational biology and bioinformatics. Tech. Rep. 2, 493–507.
Jobbágy, E.G., Sala, O.E., Paruelo, J.M., 2014. Patterns and controls of primary production in the patagonian steppe : a remote sensing approach. Ecology 83, 307–319.
Johnstone, J.F., Allen, C.D., Franklin, J.F., Frelich, L.E., Harvey, B.J., Higuera, P.E., Mack, M.C., Meentemeyer, R.K., Metz, M.R., Perry, G.L., Schoennagel, T., Turner, M.G., 2016. Changing disturbance regimes, ecological memory, and forest resilience. Front. Ecol. Environ. 14, 369–378. http://dx.doi.org/10.1002/fee.1311.
Keeley, J.E., Bond, W.J., Bradstock, R.A., Pausas, J.G., Rundel, P.W., 2011. In: Fire in Mediterranean Ecosystems, Fire in Mediterranean Ecosystems: Ecology, Evolution and Management. Cambridge University Press, Cambridge Fire in Mediterranean Ecosystems. http://dx.doi.org/10.1017/CBO9781139033091.
Keeley, J.E., Fotheringham, C.J., Baer-Keeley, M., 2005. Determinants of postfire recovery and succession in mediterranean-climate shrublands of California. Ecol. Appl. 15, 1515–1534. http://dx.doi.org/10.1890/04-1005.
Krivtsov, V., Vigy, O., Legg, C., Curt, T., Rigolot, E., Lecomte, I., Jappiot, M., Lampin-Maillet, C., Fernandes, P., Pezzatti, G.B.B., 2009. Fuel modelling in terrestrial ecosystems: an overview in the context of the development of an object-orientated database for wild fire analysis. Ecol. Modell. 220, 2915–2926. http://dx.doi.org/10.1016/j.ecolmodel.2009.08.019.
Lavorel, S., 1999. Ecological diversity and resilience of Mediterranean vegetation to disturbance. Divers. Distrib. 5, 3–13. http://dx.doi.org/10.1046/j.1472-4642.1999.00033.x.
Lee, J.-M., Lee, S.-W., Lim, J.-H., Won, M.-S., Lee, H.-S., 2014. Effects of heterogeneity of pre-fire forests and vegetation burn severity on short-term post-fire vegetation density and regeneration in Samcheok. Korean Landscape Ecol. Eng. 10, 215–228. http://dx.doi.org/10.1007/s11355-013-0214-y.
Lentile, L.B., Holden, Z.A., Smith, A.M.S., Falkowski, M.J., Hudak, A.T., Morgan, P., Lewis, S.A., Gessler, P.E., Benson, N.C., 2006. Remote sensing techniques to assess active fi re characteristics and post-fi re effects. Int. J. Wildl. Fire 15, 319–345.
Lloret, F., Calvo, E., Pons, X., Díaz-Delgado, R., 2002. Wildfires and landscape patterns in the Eastern Iberian Peninsula. Landscape Ecol. 17, 745–759. http://dx.doi.org/10.1023/A:1022966930861.
Lozano, F.J., Suárez-Seoane, S., de Luis, E., 2010. Effects of wildfires on environmental variability: a comparative analysis using different spectral indices, patch metrics and thematic resolutions. Landscape Ecol. 25, 697–710. http://dx.doi.org/10.1007/s10980-010-9453-6.
Marcos, B., Pôças, I., Gonçalves, J., Honrado, J.P., 2012. Multi-sensor assessment of trends in attributes of vegetation dynamics and ecosystem functioning derived from NDVI time series, In: Workshop Proceedings 1st EARSeL Workshop on Temporal Analysis of Satellite Images. Mykonos, Greece, pp. 254–268. doi:10.13140/2.1.2157.1524.
Marques, S., Borges, J.G., Garcia-Gonzalo, J., Moreira, F., Carreiras, J.M.B., Oliveira, M.M., Cantarinha, A., Botequim, B., Pereira, J.M.C., 2011. Characterization of wildfires in Portugal. Eur. J. For. Res. 130, 775–784. http://dx.doi.org/10.1007/s10342-010-0470-4.
Martín-Alcón, S., Coll, L., 2016. Unraveling the relative importance of factors driving post-fire regeneration trajectories in non-serotinous Pinus nigra forests. For. Ecol. Manage. 361, 13–22. http://dx.doi.org/10.1016/j.foreco.2015.11.006.
McGarigal, K., Cushman, S.A., Ene, E., 2012. FRAGSTATS v4: Spatial Pattern Analysis Program for Categorical and Continuous Maps.
Meng, R., Dennison, P.E., Huang, C., Moritz, M.A., D'Antonio, C., 2015. Effects of fire severity and post-fire climate on short-term vegetation recovery of mixed-conifer and red fir forests in the Sierra Nevada Mountains of California. Remote Sens. Environ. 171, 311–325. http://dx.doi.org/10.1016/j.rse.2015.10.024.
Metzger, M.J., Bunce, R.G.H., Jongman, R.H.G., Mücher, C.A., Watkins, J.W., Mucher, C.A., Watkins, J.W., Mücher, C.A., Watkins, J.W., 2005. A climatic stratification of the environment of Europe. Global Ecol. Biogeogr. 14, 549–563. http://dx.doi.org/10.1111/j.1466-822X.2005.00190.x.
Moreira, F., Viedma, O., Arianoutsou, M., Curt, T., Koutsias, N., Rigolot, E., Barbati, A., Corona, P., Vaz, P., Xanthopoulos, G., Mouillot, F., Bilgili, E., 2011. Landscape – wildfire interactions in southern Europe: implications for landscape management. J. Environ. Manage. 92, 2389–2402. http://dx.doi.org/10.1016/j.jenvman.2011.06.028.
Moretti, M., Legg, C., 2009. Combining plant and animal traits to assess community functional responses to disturbance. Ecography (Cop.) 32, 299–309. http://dx.doi.org/10.1111/j.1600-0587.2008.05524.x.
Morgan, P., Hardy, C.C., Swetnam, T.W., Rollins, M.G., Long, D.G., 2001. Mapping fire regimes across time and space: understanding coarse and fine-scale fire patterns. Int. J. Wildl. Fire 10, 329–342 doi:10.1071/WF01032.
Nano, C.E.M., Clarke, P.J., 2011. How do drought and fire influence the patterns of resprouting in Australian deserts? Plant Ecol. 212, 2095–2110. http://dx.doi.org/10.1007/s11258-011-9988-x.
Nardini, A., Raimondo, F., Scimone, M., Salleo, S., 2004. Impact of the leaf miner Cameraria ohridella on whole-plant photosynthetic productivity of Aesculus hippocastanum: Insights from a model. Trees – Struct. Funct. 18, 714–721. http://dx.doi.org/10.1007/s00468-004-0358-3.
Nelson, Z.J., Weisberg, P.J., Kitchen, S.G., 2014. Influence of climate and environment on post-fire recovery of mountain big sagebrush. Int. J. Wildl. Fire 23, 131. http://dx.doi.org/10.1071/WF13012.
Nunes, M.C.S., Vasconcelos, M.J., Pereira, J.M.C., Dasgupta, N., Alldredge, R.J., Rego, F.C., 2005. Land cover type and fire in portugal: do fires burn land cover selectively? Landscape Ecol. 20, 661–673. http://dx.doi.org/10.1007/s10980-005-0070-8.
Oppel, S., Strobl, C., Huettmann, F., 2009. Alternative Methods to Quantify Variable Importance in Ecology, Technical Report Number 65. University of Munich Department of Statistics.
Ordóñez, J.L., Retana, J., Espelta, J.M., 2005. Effects of tree size, crown damage, and tree location on post-fire survival and cone production of Pinus nigra trees. For. Ecol. Manage. 206, 109–117. http://dx.doi.org/10.1016/j.foreco.2004.10.067.
Oswald, B.P., Fancher, J.T., Kulhavy, D.L., Reeves, H.C., 1999. Classifying fuels with aerial photography in East Texas. Int. J. Wildl. Fire 9, 109–113. http://dx.doi.org/10.1071/WF00002.
Pausas, J.G., 2004. Changes in fire and climate in the eastern Iberian Peninsula (Mediterranean Basin). Clim. Change 63, 337–350. http://dx.doi.org/10.1023/B:CLIM.0000018508.94901.9c.
Pausas, J.G., Bradstock, R.A., 2007. Fire persistence traits of plants along a productivity and disturbance gradient in mediterranean shrublands of south-east Australia. Glob. Ecol. Biogeogr. 16, 330–340. http://dx.doi.org/10.1111/j.1466-8238.2006.00283.x.
Pausas, J.G., Lloret, F., 2007. Spatial and temporal patterns of plant functional types under simulated fire regimes. Int. J. Wildl. Fire 16, 484–492. http://dx.doi.org/10.1071/WF06109.
Pearson, R.K., 2002. Outliers in process modeling and identification. IEEE Trans. Control Syst. Technol. 10, 55–63. http://dx.doi.org/10.1109/87.974338.
Pereira, J.M.C.J., Carreiras, J.J.M.B., Silva, J.J.M.N., Vasconcelos, M.J., MJP, 2006. Alguns conceitos básicos sobre os fogos rurais em Portugal, In: Incêndios Florestais Em Portugal: Caracterização, Impactes E Prevenção. ISA press, pp. 133–161.
Pereira, J.M.C., Carreiras, J.M.B., Vasconcelos, M.J.P., 1998. Exploratory data analysis of the spatial distribution of wildfires in Portugal, 1980–1989. Geograph. Sys. 5 (4), 355–390.
Pereira, J.M.C., Santos, M.T., 2003. Cartografiadas Áreas Queimadas e do Risco de Incêndio em Portugal Continental (1990–1999). Direção-Geral das Florestas, Lisboa, Portugal.
Pettorelli, N., Vik, J.O., Mysterud, A., Gaillard, J.-M., Tucker, C.J., Stenseth, N.C., 2005. Using the satellite-derived NDVI to assess ecological responses to environmental change. Trends Ecol. Evol. 20, 503–510. http://dx.doi.org/10.1016/j.tree.2005.05.011.
Pettorelli, N., Wegmann, M., Skidmore, A., Mücher, S., Dawson, T.P., Fernandez, M., Lucas, R., Schaepman, M.E., Wang, T., O'Connor, B., Jongman, R.H.G., Kempeneers, P., Sonnenschein, R., Leidner, A.K., Böhm, M., He, K.S., Nagendra, H., Dubois, G., Fatoyinbo, T., Hansen, M.C., Paganini, M., de Klerk, H.M., Asner, G.P., Kerr, J.T., Estes, A.B., Schmeller, D.S., Heiden, U., Rocchini, D., Pereira, H.M., Turak, E., Fernandez, N., Lausch, A., Cho, M.A., Alcaraz-Segura, D., McGeoch, M.A., Turner, W., Mueller, A., St-Louis, V., Penner, J., Vihervaara, P., Belward, A., Reyers, B., Geller, G.N., 2016. Framing the concept of satellite remote sensing essential biodiversity variables: challenges and future directions. Remote Sens. Ecol. Conserv. 2, 122–131. http://dx.doi.org/10.1002/rse2.15.
R Development Core and Team, 2016. R: A Language and Environment for Statistical Computing. R Foundation for Statistical Computing, Vienna.
Riaño, D., Chuvieco, E., Salas, J., Palacios-Orueta, A., Bastarrika, A., 2002. Generation of fuel type maps from Landsat TM images and ancillary data in Mediterranean ecosystems. Can. J. For. Res. 32, 1301–1315. http://dx.doi.org/10.1139/x02-052.
Rogers, B.M., Randerson, J.T., Bonan, G.B., 2012. High latitude cooling associated with landscape changes from North American boreal forest fires. Biogeosci. Discuss. 9, 12087–12136. http://dx.doi.org/10.5194/bgd-9-12087-2012.
Román-Cuesta, R.M., Gracia, M., Retana, J., 2009. Factors influencing the formation of unburned forest islands within the perimeter of a large forest fire. For. Ecol. Manage. 258, 71–80. http://dx.doi.org/10.1016/j.foreco.2009.03.041.
Theil, H., 1950. A rank-invariant method of linearand polynomial regression analysis, Part 3. Proceedings of KoninalijkeNederlandse Akademie van Weinenschatpen 53, 1397–1412.
Schneider, P., Roberts, D.A., Kyriakidis, P.C., 2008. A VARI-based relative greenness from MODIS data for computing the Fire Potential Index. Remote Sens. Environ. 112, 1151–1167. http://dx.doi.org/10.1016/j.rse.2007.07.010.
Shatford, J.P.A., Hibbs, D.E., Puettmann, K.J., 2007. Conifer regeneration after forest fire in the Klamath-Siskiyous: how much, how soon? J. For. 105, 139–146.
Shryock, D.F., Esque, T.C., Chen, F.C., 2015. Topography and climate are more important drivers of long-term, post-fire vegetation assembly than time-since-fire in the Sonoran Desert. U.S. J. Veg. Sci. 26, 1134–1147. http://dx.doi.org/10.1111/jvs.12324.
Solano, R., Didan, K., Jacobson, A., Huete, A., 2010. MODIS Vegetation Indices (MOD13) C5 User's Guide. Terrestrial Biophysics and Remote Sensing Lab. The University of Arizona.
Strobl, C., Zeileis, A., 2008. Danger: High Power! – Exploring the Statistical Properties of a Test for Random Forest Variable Importance.
Tachikawa, T., Kaku, M., Iwasaki, A., 2011. ASTER GDEM Version 2 Validation Report, In: International Geoscience and Remote Sensing Symposium (IGARSS). pp. 1–24.
Tang, G.H., Rabie, a B.M., Hägg, U.,, 2004. Indian hedgehog: a mechanotransduction mediator in condylar cartilage. J. Dent. Res. 83, 434–438. http://dx.doi.org/10.1177/154405910408300516.
Tonbul, H., Kavzoglu, T., Kaya, S., 2016. XLI-B8 In: Assessment of Fire Severity And Post-Fire Regeneration Based On Topographical Features Using Multitemporal Landsat Imagery: A Case Study In Mersin, Turkey. ISPRS – Int. Arch. Photogramm. Remote Sens. Spat. Inf. Sci., pp. 763–769. http://dx.doi.org/10.5194/isprsarchives-XLI-B8-763-2016.
Turner, M.G., Romme, W.H., 1994. Landscape dynamics in crown fire ecosystems. Landscape Ecol. 9, 59–77. http://dx.doi.org/10.1007/BF00135079.
Van Leeuwen, W.J.D., Casady, G.M., Neary, D.G., Bautista, S., Alloza, J.A., Carmel, Y., Wittenberg, L., Malkinson, D., Orr, B.J., 2010. Monitoring post-wildfire vegetation response with remotely sensed time-series data in Spain, USA and Israel. Int. J. Wildl.

Fire 19, 75–93. http://dx.doi.org/10.1071/WF08078.
Vaughan, C.L., 1982. Smoothing and differentiation of displacement-time data: an application of splines and digital filtering. Int. J. Biomed. Comput. 13, 375–386. http://dx.doi.org/10.1016/0020-7101(82)90003-4.
Veraverbeke, S., Lhermitte, S., Verstraeten, W.W., Goossens, R., 2011. A time-integrated MODIS burn severity assessment using the multi-temporal differenced normalized burn ratio (dNBRMT). Int. J. Appl. Earth Obs. Geoinf. 13, 52–58. http://dx.doi.org/10.1016/j.jag.2010.06.006.
Wang, Q., Adiku, S., Tenhunen, J., Granier, A., 2005. On the relationship of NDVI with leaf area index in a deciduous forest site. Remote Sens. Environ. 94, 244–255. http://dx.doi.org/10.1016/j.rse.2004.10.006.
White, J.C., Wulder, M.A., Hermosilla, T., Coops, N.C., Hobart, G.W., 2017. A nationwide annual characterization of 25 years of forest disturbance and recovery for Canada using Landsat time series. Remote Sens. Environ. 194, 303–321. http://dx.doi.org/10.1016/j.rse.2017.03.035.
Xu, Q.S., Liang, Y.Z., Du, Y.P., 2004. Monte Carlo cross-validation for selecting a model and estimating the prediction error in multivariate calibration. J. Chemom. 18, 112–120. http://dx.doi.org/10.1002/cem.858.